

Received 3 June 2018; revised 20 August 2018 and 4 October 2018; accepted 28 October 2018.
Date of publication 1 November 2018; date of current version 15 November 2018.

Digital Object Identifier 10.1109/JTEHM.2018.2879085

Sleep Apnea Syndrome Sensing at C-Band

XIAODONG YANG¹, (Senior Member, IEEE), DOU FAN¹, AIFENG REN¹,
NAN ZHAO¹, ZHIYA ZHANG¹, FANGMING HU¹, WEIGANG WANG²,
MASOOD UR REHMAN³, (Senior Member, IEEE),
AND JIE TIAN^{4,5}, (Fellow, IEEE)

¹School of Electronic Engineering, Xidian University, Xi'an 710071, China

²Northwest Women's and Children's Hospital, Xi'an Jiaotong University, Xi'an 710061, China

³School of Computer Science and Electronic Engineering, University of Essex, Colchester CO4 3SQ, U.K.

⁴School of Life Sciences and Technology, Xidian University, Xi'an 710126, China

⁵Institute of Automation, Chinese Academy of Sciences, Beijing 100190, China

CORRESPONDING AUTHOR: J. TIAN (jaytian99@gmail.com)

This work was supported in part by the National Natural Science Foundation of China under Grant 61671349, Grant 61301175, and Grant 61601338, in part by the China Postdoctoral Science Foundation Funded Project under Grant 2018T111023, in part by the International Scientific and Technological Cooperation and Exchange Projects in Shaanxi Province under Grant 2017KW-005, and in part by the Fundamental Research Funds for the Central Universities under Grant JB180205.

ABSTRACT A non-intrusive sleep apnea detection system using a C-Band channel sensing technique is proposed to monitor sleep apnea syndrome in real time. The system utilizes perturbations of RF signals to differentiate between patient's breathing under normal and sleep apnea conditions. The peak distance calculation is used to obtain the respiratory rates. A comparison of the datasets generated by the proposed method and a wearable sensor is made using a concordance correlation coefficient to establish its accuracy. The results show that the proposed sensing technique exhibits high accuracy and robustness, with more than 80% concordance with the wearable breathing sensor. This method is, therefore, a good candidate for the real-time wireless detection of sleep apnea.

INDEX TERMS Sleep detection, C-Band sensing, peak distance calculation, concordance correlation coefficient.

I. INTRODUCTION

Sleep Apnea Syndrome (SAS) is a common clinical syndrome that causes frequent pauses in the patient's breathing. SAS occurs due to apnea and blood oxygen desaturation during sleep. There are two basic types of SAS: Central Sleep Apnea and Obstructive Sleep Apnea. Central Sleep Apnea occurs due to the brain failing to send the right signals to the muscles that control breathing. Obstructive Sleep Apnea occurs due to a blockade of the upper airway. Sleep Apnea Syndrome, whether obstructive or central, can lead to high blood pressure, coronary heart disease, life-threatening cardiac arrhythmias, systemic or pulmonary hypertension, arterial blood gas abnormalities, chronic respiratory failure, sleep disturbances narcolepsy, excessive daytime somnolence, sexual dysfunction and mental decline [1]. In general, these symptoms become obvious before the age of 40 years old and cluster within a few years. As an underlying physical disease, SAS is difficult to detect easily during sleep and poses a significant challenge to health.

Polysomnography (PSG) is the most widely used medical test to monitor respiratory events and diagnose sleep-related breathing disorders, including SAS. PSG is performed while the subject is asleep and analyses the patient's respiratory rate (RR), heart rate (HR), electroencephalogram (EEG), electrocardiogram (ECG), electrooculogram (EOG), electromyography (EMG), and oxygen saturation (SpO₂) level [2]. However, very particular measurement requirements limit the ability of PSG to reflect the conditions of a regular night sleep in the subject's home [3], and it is very expensive. Moreover, PSG requires specific equipment that is available only in a handful of hospitals and institutions.

Researchers have proposed many different approaches for SAS detection to overcome the drawbacks of PSG. Contact sensor based detection methods were proposed in [4]–[7]. For example, an off-the-shelf wearable single sensor [4] was used to detect the severity of SAS according to the instantaneous heart rate (IHR) and blood oxygen saturation (SpO₂) levels. A gas sensor array was used to screen SAS, and the

performance of the method is susceptible to a number of environmental and metabolic variables [5]. Hernandez *et al.* [6] estimated the heart and breathing rates by using accelerometer and gyroscope sensors worn on the patient's wrist. Kukkapalli *et al.* [7] used a wearable micro-radar to monitor breathing behaviour. It is worth mentioning that these systems and approaches are contact based. An e-textile pressure sensitive bed sheet was also used to measure the breathing rate by analysing the time-stamped pressure distribution sequences in [8]. However, this technique requires the subject to lay flat and fails when the subject is positioned in other position. Non-invasive breathing rate monitoring and apnea detection were achieved in [9] and [10]. In [9], received signal strength (RSS) is utilized to extract respiration rate. However, the quantization errors and electronic noise may reduce the accuracy of respiratory rate estimation. In [10], frequency modulated continuous wave (FMCW) radar was used to monitor a person's breathing rate; the system contains some specialized devices. In this paper, we propose a SAS detection system using wireless channel information at C-band.

This non-intrusive method detects sleep apnea accurately in real-time through observation of slight changes in the wireless channel caused by the breathing pattern and chest movements. Following the introduction, this paper is organized into six sections. Section II provides the justification for the use of C-band frequencies for the proposed technique. Section III discusses the data processing methods used in the proposed technique, while Section IV provides the details of the monitoring system. The results are analysed in Section V, and the conclusions are drawn in Section VI.

II. C-BAND FREQUENCIES

Fifth generation wireless systems, abbreviated as 5G, meet the upcoming telecommunications standard, which has evolved to substantially enhance the currently used 4G/IMT-Advanced standard [11]. 5G aims to provide high data rates and higher capacity than 4G in three ways: enhanced mobile broadband (eMBB), massive machine type communication (mMTC) and ultra reliable low latency communications (URLLC) [12]. With the advent of 5G networks, data traffic is estimated to grow exponentially, with an influx of new applications. Recently, the Ministry of Industry and Information Technology of the People's Republic of China has published a notification to allocate frequencies of 3.3 GHz~3.6 GHz and 4.8 GHz~5.0 GHz for IMT2020, popularly known as 5G [13].

The C-band refers to the frequency band of 4.8GHz. To make our proposed SAS detection system compatible with current and future 5G applications, a C-band frequency of 4.8 GHz was selected as the operating frequency of the transmitter.

In [14], a portable noncontact heartbeat and respiration monitoring system operating in 5GHz was reported, and the proposed system can be used for various applications; Li *et al.* [15] designed a 5GHz double-sideband radar chip

for non-contact vital sign detection, the system can avoid null detection point by frequency tuning. These well-designed radar systems contain some specialized and sophisticated devices and the vital data of the patients can be recorded.

III. DATA PROCESSING METHODS

A. PEAK DISTANCE CALCULATION METHOD

The breathing rate is a key indicator of breathing-related sleep disorders. Figure 1 presents a respiratory signal of a one-minute duration observed for one subject. The signal has a wave-like pattern. The zero-line segmentation is selected to separate the signal into positive and negative parts.

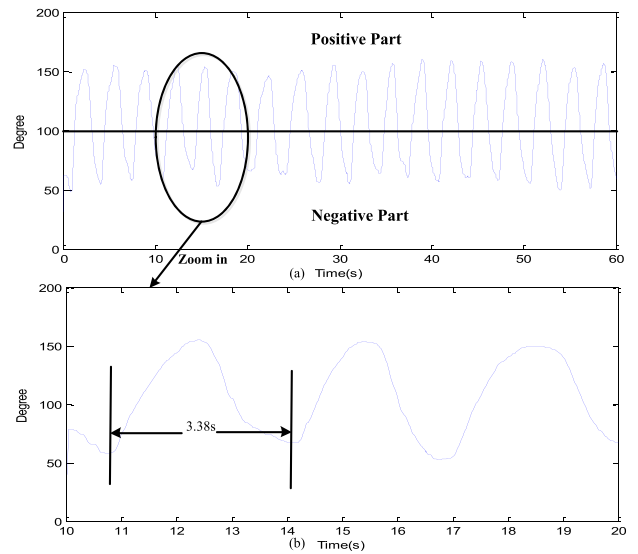


FIGURE 1. Respiratory signal observed for a subject; (a) complete signal of a one minute duration, (b) zoomed-in portion of the respiration signal.

As shown, the respiratory signal in Figure 1(a) has 18 wave crests and troughs over a one minute observation duration. The residual values for the two wave crests or troughs can be calculated as follows:

$$R = \frac{1}{N-1} \sum_{n=1}^{N-1} [y(n+1) - x(n)] \quad (1)$$

where $x(n)$ and $y(n)$ are the time duration between two consecutive wave crests/troughs, N is the number of crests/troughs, and R is the calculated breathing rate. A breathing rate of 3.3 s is obtained for the observed signal through this expression. For verification, a zoomed-in section of the signal is used, as shown in Figure 1(b). The distance between two consecutive wave troughs is shown to be 3.38 s. It is therefore evident that an accurate breathing rate can be determined by employing the peak distance calculation method.

B. CONCORDANCE CORRELATION COEFFICIENT

The concordance correlation coefficient is an index that describes the reproducibility between two datasets [16]. Normal breathing and apnea conditions for the sleeping subjects are observed through both the proposed C-band sensing system and a wearable respiration sensor simultaneously.

The concordance correlation coefficient is then used to evaluate the agreement between the two measurements and establish the accuracy of the proposed technique.

The concordance correlation coefficient is based on the Pearson correlation coefficient. The Pearson correlation coefficient is a measure of the strength and direction of the linear relationship between two variables. The two zero-mean, real-valued random variables Y_1 and Y_2 , which represent the two signals, are defined as [17]:

$$\rho(a, b) = \frac{E(Y_1 Y_2)}{\sigma_1 \sigma_2} \quad (2)$$

where $E(Y_1 Y_2)$ is the cross-correlation between Y_1 and Y_2 and $\sigma_1^2 = E(Y_1^2)$ and $\sigma_2^2 = E(Y_2^2)$ are the variance of Y_1 and Y_2 , respectively.

Considering pairs of samples $(Y_{i1}, Y_{i2}), i = 1, 2, \dots, n$, independently selected from a bivariate population, their means are μ_1 and μ_2 and their covariance matrix is [16]:

$$\begin{pmatrix} \sigma_1^2 & \sigma_{12} \\ \sigma_{12} & \sigma_2^2 \end{pmatrix} \quad (3)$$

The value of the squared difference describes the degree of concordance between Y_1 and Y_2 :

$$\begin{aligned} E[(Y_1 - Y_2)^2] &= (\mu_1 - \mu_2)^2 + (\sigma_1^2 + \sigma_2^2 - 2\sigma_{12}) \\ &= (\mu_1 - \mu_2)^2 + (\sigma_1 - \sigma_2)^2 + 2(1 - \rho)\sigma_1\sigma_2 \end{aligned} \quad (4)$$

where ρ is the Pearson correlation coefficient.

The concordance correlation coefficient is, therefore, defined as:

$$\rho_c = 1 - \frac{E[(Y_1 - Y_2)^2]}{\sigma_1^2 + \sigma_2^2 + (\mu_1 - \mu_2)^2} \quad (5)$$

and,

$$\rho_c = \frac{2\sigma_{12}}{\sigma_1^2 + \sigma_2^2 + (\mu_1 - \mu_2)^2} = \rho C_b \quad (6)$$

where,

$$\begin{aligned} C_b &= [(v + 1/v + u^2)/2]^{-1}, \\ v &= \sigma_1/\sigma_2, \\ u &= (\mu_1 - \mu_2)/\sqrt{\sigma_1\sigma_2}. \end{aligned}$$

The concordance correlation coefficient, ρ_c , is required to fulfil the following condition:

$$-1 \leq -|\rho| \leq \rho_c \leq |\rho| \leq 1 \quad (7)$$

IV. SYSTEM DESIGN

This section discusses the design and architecture of the proposed C-band sensing system for SAS detection.

A. PRELIMINARIES

Every wireless channel has a unique fingerprint. The Wireless Channel Information (WCI) records the channel attenuation factor of the individual paths in the process of signal transmission and reception. The Wireless Channel Information for a certain wireless link is expressed as follows:

$$Y(t) = \text{WCI} \times X(t) + n \quad (8)$$

where $X(t)$ is the transmitted signal, $Y(t)$ is the received signal, and n is Gaussian white noise. The wireless channel is typically modelled using the Channel Impulse Response (CIR) to account for multi-path propagation. Considering a linear time invariant system, the CIR is expressed as [18]:

$$h(\tau) = \sum_{i=1}^N a_i e^{-j\theta_i \delta(\tau - \tau_i)} \quad (9)$$

where α_i , θ_i , and τ_i indicate the amplitude, phase and time delay of the i^{th} path, respectively. N denotes the total number of propagation paths, while $\delta(\tau)$ is the Dirac delta function. Each impulse response describes a delayed multi-path component multiplied by the corresponding amplitude and phase information.

In the frequency domain, the multi-path propagation manifests the frequency selective fading. The Channel Frequency Response (CFR), therefore, can be used to describe the effects of the echo pathways. For an infinite bandwidth, CFR can be found using the Fourier transform of CIR, while CIR is the inverse transform of CFR, expressed as:

$$\text{CFR}(\omega) = F[\text{CIR}(t)] = \int_{-\infty}^{\infty} \text{CIR}(t)e^{-j\omega t} dt \quad (10)$$

$$\text{CIR}(t) = F^{-1}[\text{CFR}(\omega)] = \frac{1}{2\pi} \int_{-\infty}^{\infty} \text{CFR}(\omega)e^{j\omega t} d\omega \quad (11)$$

The experimental set-up used for sleep apnea detection in this study is illustrated in Figure 2. The microwave sensing platform was used to conduct the experiment in a room with the size 5m × 7m. The omnidirectional antennas, whose height is 70cm, were placed vertically to the ground. The subjects lay on a bed with the height of 50cm. The transmitter (Tx) and the receiver (Rx) were placed at the two sides of the bed and the system worked at 4.8 GHz. The distance between Tx and Rx is 2m. The receiver is connected to a computer through an embedded data collection system. The ground truths of breathing rate are monitored by the HKH-11C respiration sensor. We repeated the experiment on five different subjects and the subject details are given in Table 1.

After most of the electromagnetic waves enter the absorbing material, the electromagnetic wave energy is changed into heat energy, which is depleted slowly into the absorbing material. A microwave absorbing material is placed at the sides of the room to reduce the effects of the surroundings and minimize multi-path propagation for enhanced accuracy.

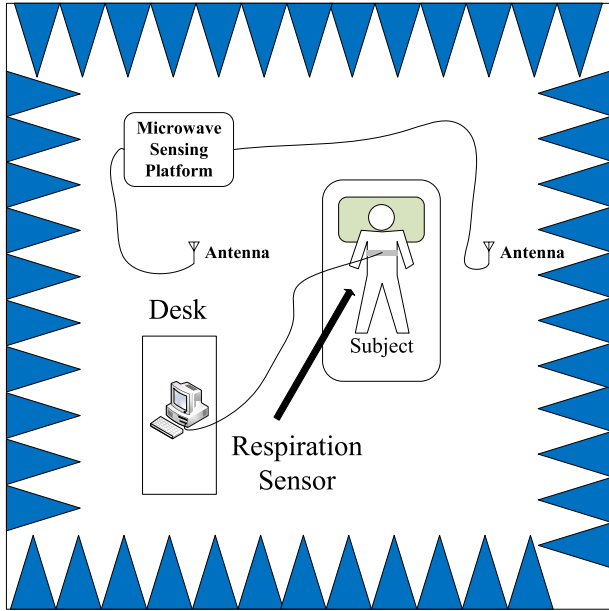


FIGURE 2. Experimental set-up for the detection of sleep apnea using the C-Band sensing technique.

TABLE 1. Subject data used for the experiment.

Subject-ID	Subject weight (in Kg)	Subject height (in cm)
1	74	183
2	52	167
3	85	178
4	61	173
5	67	175

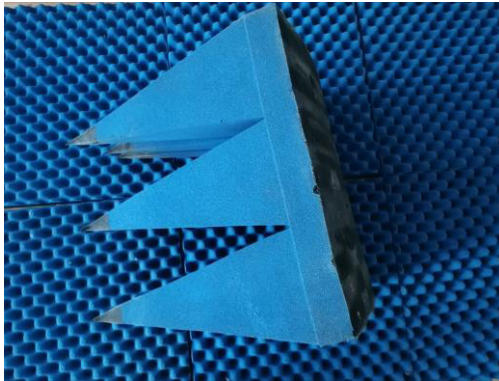


FIGURE 3. Pyramidal absorbing material.

This set-up is a composite of adsorbent and multifarious materials that transforms incident electromagnetic waves into heat energy, which is then depleted slowly into the absorbent, resulting in almost no reflection. One of the most widely used type of material, ferrite absorption material (shown in Figure 3), is employed in this study.

Wireless transmission uses Orthogonal Frequency Division Multiplexing (OFDM), in which data bits are transmitted in parallel through multiple orthogonal subcarriers. A group of 30 subcarriers carrying amplitude information are

received as one WCI packet (in the form of CFR), which is expressed as:

$$CFR_n = [[h_1, h_2, h_3, \dots, h_k,]] \quad (12)$$

where $h_i(n)$ indicates the CFR of the n^{th} subcarrier. To analyse the CFR data stream considering the time history, all of the CFR_m values obtained at different times are combined:

$$CFR_{\text{time_history}} = [[CFR(1), CFR(2), CFR(3), \dots, CFR(m)]] \quad (13)$$

B. SYSTEM OVERVIEW

The proposed C-band system observes wireless channel variations caused by changing chest heights due to normal and sleep apnea breathing patterns. Simultaneous measurements are carried out using a wearable respiratory sensor to benchmark the proposed system. Figure 4 illustrates the overall system. The proposed system consists of four modules for respiratory signal acquisition, data processing, normal breath detection and SAS event identification.

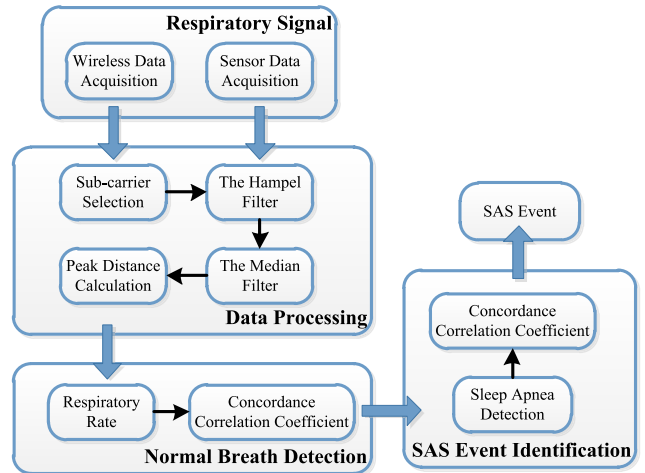


FIGURE 4. Overview of the proposed system architecture.

The respiratory signal acquisition module gathers the unprocessed breathing data through C-band sensing and a wearable respiration sensor. The data processing module then selects the subcarriers that contain the best CFR information out of 30 OFDM subcarriers. To rectify the influence of various external factors, the elimination of outliers is necessary. The Hampel filter, which removes outliers based on their position relative to a good observation model, is used for this purpose [19]. A smooth wave pattern of the observed signals is achieved using a median filter.

The normal breath detection module utilizes the Peak Distance Calculation method to acquire the respiratory rate. Additionally, the two data sets are compared to find the concordance correlation coefficient. Then, the accuracy is calculated using the formula below:

$$A = 1 - \frac{|f_s - f_t|}{f_s} \times 100\% \quad (14)$$

where A is the accuracy rate, f_s is the respiratory rate measured by the contact respiratory sensor, and f_t is the respiratory rate detected by the proposed system.

Finally, sleep apnea will be determined by the SAS event identification module via the variation of wireless channel information. If the wireless channel information is initially periodic but then become constant for no less than 10 seconds, an apnea occurs.

V. EXPERIMENTAL RESULTS

Chest movements of a subject are observed for one minute using both the C-band system and a wearable respiratory sensor. The data are then analysed to first identify the normal breathing pattern and then to detect any SAS event. The accuracy and robustness of the proposed system is discussed.

A. NORMAL BREATH DETECTION

The respiratory rate is an important diagnostic indicator of potential respiratory dysfunction in acutely sick patients. The respiratory rate is measured by counting the number of chest rises for one minute when a person is at rest.

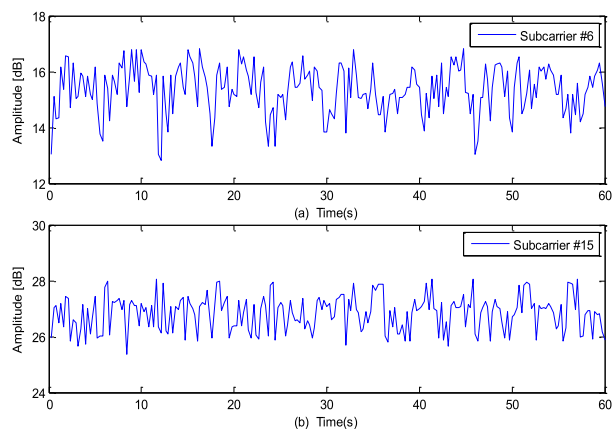


FIGURE 5. Wireless channel information sequences of subcarrier #6 and #15.

In this study, C-band sensing is used to measure the respiratory rate via wireless channel information. Wireless channel information data from all 30 subcarriers is measured. The wireless channel information sequences of subcarrier #6 and #15 are plotted in Figure 5. It should be noted that despite having different profiles, both of these responses are obtained under exactly the same conditions because the amplitudes of different subcarriers have distinct sensitivities for chest movement. It is therefore important to choose the subcarrier with the best response. The variance of wireless channel information amplitude in a moving time window is used to quantify the subcarrier’s sensitivity. The variances of 30 subcarriers are shown in Fig. 6. The subcarrier with higher variance should be selected since greater variance indicates higher sensitivity. Thus we use maximum variance method to select subcarrier. Based on this selection criterion, the wireless channel information sequence for the 6th subcarrier is shown in Figure 7(a). There are

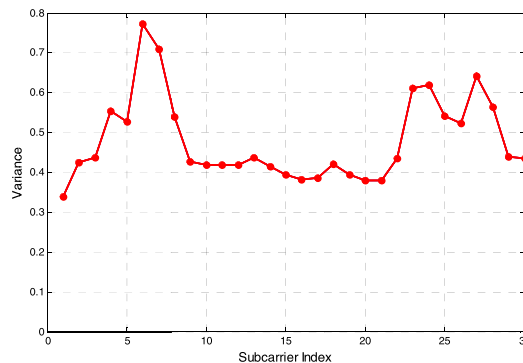


FIGURE 6. Variance of 30 subcarriers.

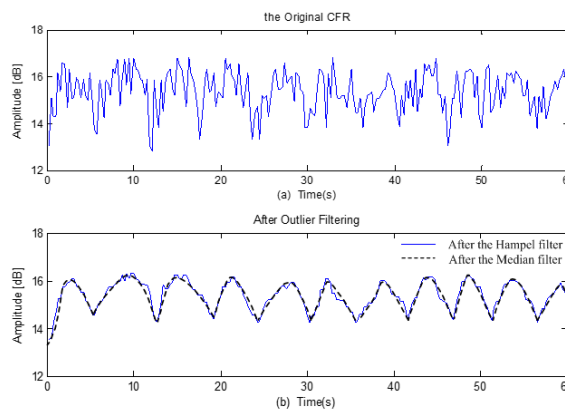


FIGURE 7. Wireless channel information sequences of subcarrier #6 when the subject is breathing normally; (a) original CFR, (b) filtered CFR after using the Hampel and median filters.

approximately 11 wave-like patterns in this response. However, these wave-like patterns are not obvious due to the presence of outliers, which necessitates filtering of outliers.

The Hampel filter is used to eliminate outliers. This filtering specifies a lower and upper bound that depend on the sample size and chosen value of α_N . The value of α_N is given by the statistician. In general, for a given α , the value of α_N is computed by:

$$\alpha_N = 1 - (1 - \alpha)^{1/N} \tag{15}$$

where N is the sample size.

The median filter is then used to remove noise and produce a smoother waveform. The median filter replaces each signal value with the median of the neighbouring values. Figure 7(b) shows the CFR after using the Hampel filter and median filter. The usefulness of the two filters is evident from these results, as the breathing pattern closely approximates a periodic sine wave.

The breathing signal recorded using the wearable respiratory sensor is shown in Figure 8(a). It is observed that there are no outliers present in this breathing pattern. Therefore, only the median filter is applied to achieve a smoother sine wave-like pattern, as shown in Figure 8(b).

The data obtained through the two methods are then evaluated for respiratory rate analysis. Wave periodicity is

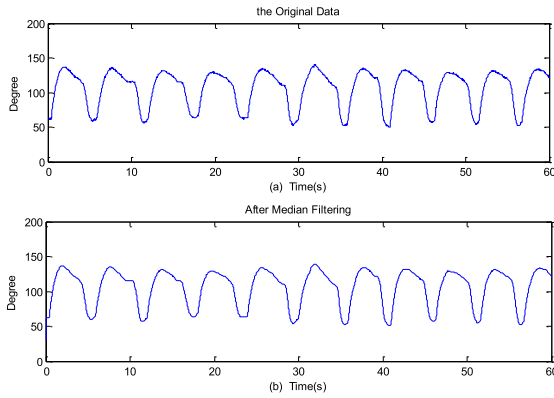


FIGURE 8. Breathing pattern for the normal breathing condition observed using a wearable respiratory sensor; (a) original data, (b) data after using the median filter.

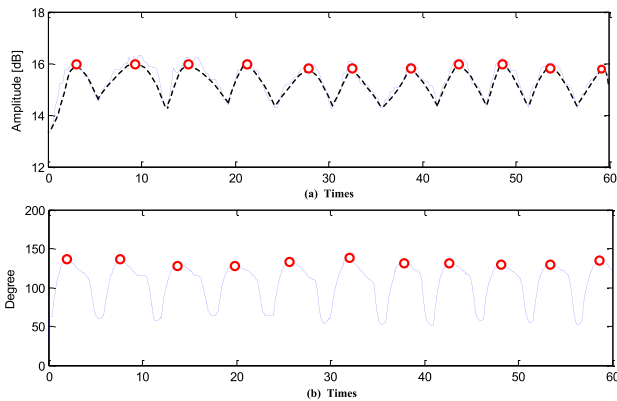


FIGURE 9. Respiratory rate analysis; (a) filtered CFR data, (b) filtered sensor data.

determined from the filtered breathing patterns, as shown in Figure 9. The Peak Distance Calculation method is used to calculate the respiratory rate. The results shown in Figure 9(a) show that there are 11 wave crests (red circles in Figure 9(a)) in one minute for the data obtained by means of the C-band sensing technique, giving a respiratory rate of 5.5 s. For the respiratory sensor data shown in Figure 9(b), a total of 11 wave peaks (red circles in Figure 9(b)) exist over a one minute long signal, for a respiratory rate of 5.5 s.

The accuracy of the proposed C-band sensing technique compared to that of the respiratory sensor is determined by calculating the concordance correlation coefficient and detection accuracy rate. Using the two filtered data sequences shown in Figure 9, the value of the concordance correlation coefficient appears to be 0.805 from Equation 5 or 6. And the detection accuracy rate calculated by Equation 14 is up to 94.3%; therefore, it can be concluded that the proposed C-band sensing technique is very efficient for detection of the breathing pattern and the respiratory rate.

B. SAS EVENT IDENTIFICATION

The C-band sensing technique is then used to identify SAS events, and its performance is compared with that of a standard respiratory sensor. Sleep apnea is characterized

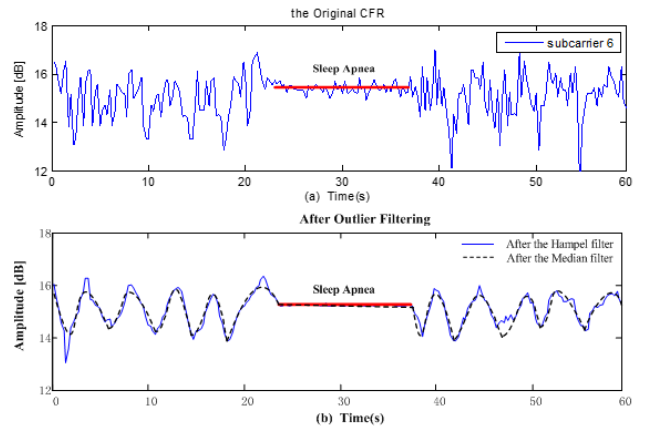


FIGURE 10. Wireless channel information sequences on subcarrier #6 showing the occurrence of a SAS event; (a) original CFR, (b) filtered CFR.

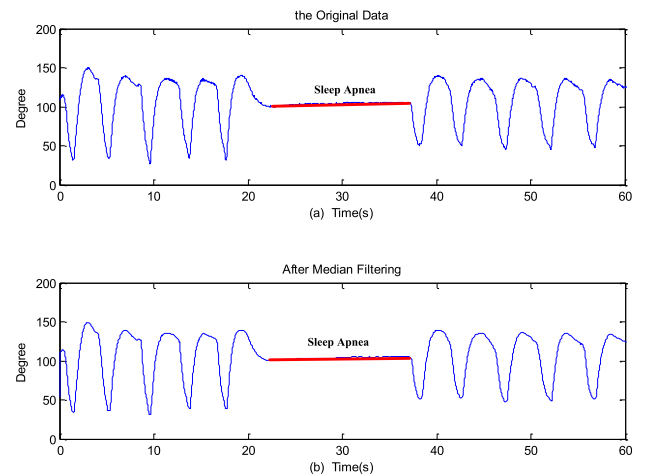


FIGURE 11. Pattern from using the contact respiratory sensor when the subject is breathing; (a) original data, (b) data after using the median filter.

by pauses in breathing or periods of shallow breathing during sleep. Each of these pauses can last for at least 10 seconds [20]. When an apnea event occurs, the chest movement caused by breathing disappears, resulting in changes to the measured respiratory amplitude.

The wireless channel information is again noted over a one minute duration. The best response of the wireless channel information of the 30 subcarriers assessed was observed for subcarrier #6, as shown in Figure 10. Figure 10(a) shows that the subject was breathing normally for 22s. A sleep apnea event occurred at 23s, making the subject stop breathing for the next 10s. The subject then started breathing again at approximately 37s. Figure 10(b) shows the filtered CFR after using the Hampel filter and median filter to remove outliers and obtain a smooth data sequence.

The breathing signal recorded by the wearable respiratory sensor is shown in Figure 11(a). Figure 11(b) depicts a smoother pattern obtained via median filtering. The apnea event is evident from these measurements as well. The subject is breathing normally from 0 to 23s. The constant amplitude level for the next 14 seconds (from 23s to 37s) shows that

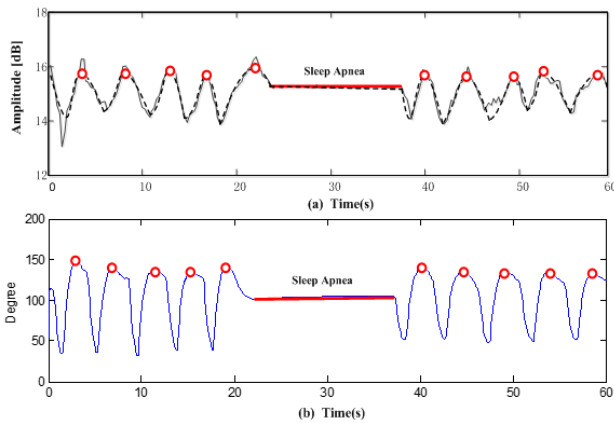


FIGURE 12. SAS event identification; (a) filtered CFR data, (b) filtered sensor data.

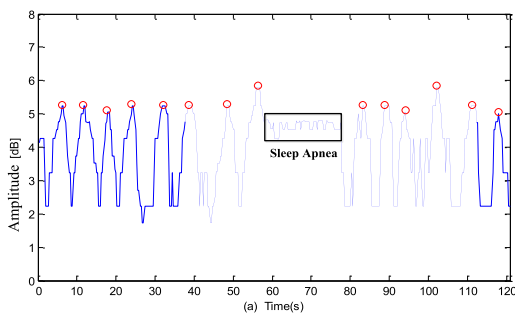


FIGURE 13. SAS event identification for Subject 2.

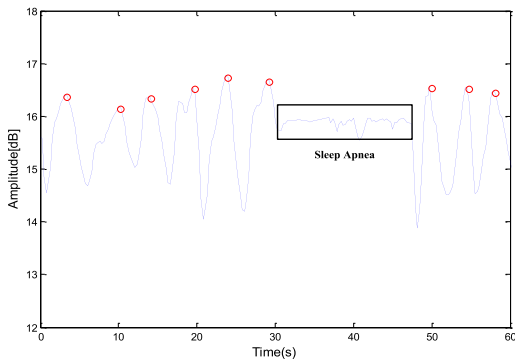


FIGURE 14. SAS event identification for Subject 3.

the subject is experiencing a sleep apnea episode. When the apnea is over at 37s, the subject started breathing normally again.

Figure 12 shows the wave periodicity in the two filtered breathing patterns. It is quite clear that 10 wave peaks (red circles) and an apnea were detected. The respiratory rate for the C-band sensed data shown in Figure 12(a) through Peak Distance Calculation method appears to be 4.7s. The respiratory rate for the respiratory sensor data shown in Figure 12(b) is found to be 4.5s, which shows a close agreement between the two methods.

The usefulness of the system has also been proved by considering some other subjects, as shown in Fig. 13 and 14, the SAS symptom was clearly detected. The periods of the apnea for the subjects are almost the same.

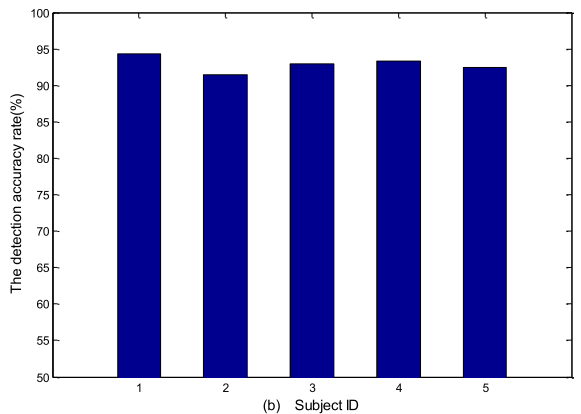
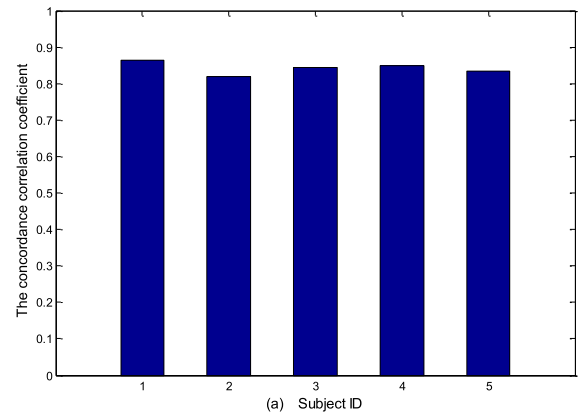


FIGURE 15. The detection results of five subjects; (a) the concordance correlation coefficients, (b) the detection accuracy rates.

To establish the accuracy level of the proposed C-band sensing scheme, the concordance correlation coefficient and detection accuracy rate are calculated using two data sets. The values are 0.865 and 94.3%, respectively. The results of the proposed method and the respiratory sensor show very good consistency.

The concordance correlation coefficients and detection accuracy rate of five subjects are given in Fig. 15(a) and 15(b), respectively. All of the concordance correlation coefficients are above 0.8 and all accuracy of detection are more than 90%; the effectiveness of the system has been fully verified.

Comparing these results with other detecting results generated by specialized radar systems [14], [15], our precision is high enough, and since the facilities included are not purpose-designed, easiness to be implemented is also the important characteristic of the system.

Also, these results demonstrate the effectiveness of the system. The system is non-contact and the patient will have better comfort, the breathing activity will not be affected by the cables, etc. Besides, the system is real time and the experimental setup is flexible; thus the technique is adaptive to the environment to some extent.

VI. CONCLUSION

In this paper, we proposed a real-time and non-intrusive sleep apnea detection system using C-band wireless sensing.

The system makes use of a wireless transmitter and receiver operating at the 4.8 GHz frequency using OFDM. The system detects the breathing activities of a patient by means of a radio signal indicating variations in the wireless channel information due to varying chest movements for normal breathing and pauses during apnea episodes. Raw data for the most sensitive subcarrier was processed using Hampel and median filtering to remove outliers and noise from the channel response. The performance and accuracy of the proposed system was established through a comparison of data in the form of a concordance correlation coefficient with standard respiratory sensor measurements. A high correlation of more than 0.8 between the two data sets was observed. It was observed through the presented results and analysis that the proposed sensing technique had high accuracy levels and efficiently detected SAS episodes in real time. Moreover, the proposed sensing technique offers the advantages of non-intrusiveness, flexibility, making it a well suited alternative to traditional techniques.

REFERENCES

- [1] B. A. Chaudhary and J. W. Speir, Jr., "Sleep apnea syndromes," *Southern Med. J.*, vol. 75, no. 1, pp. 39–45, 1982.
- [2] C. A. Kushida, "Practice parameters for the indications for polysomnography and related procedures: An update for 2005," *Sleep*, vol. 28, no. 4, pp. 499–523, 2005.
- [3] K. E. Bloch, "Polysomnography: A systematic review," *Technol. Health Care*, vol. 5, no. 4, pp. 285–305, 1997.
- [4] R. K. Pathinarupothi, J. D. Prathap, E. S. Rangan, E. A. Gopalakrishnan, R. Vinaykumar, and K. P. Soman, "Single sensor techniques for sleep apnea diagnosis using deep learning," in *Proc. IEEE Int. Conf. Healthcare Inform. (ICHI)*, Aug. 2017, pp. 524–529.
- [5] R. A. Incalzi *et al.*, "Comorbidity modulates non invasive ventilation-induced changes in breath print of obstructive sleep apnea syndrome patients," *Sleep Breathing*, vol. 19, no. 2, pp. 623–630, 2015.
- [6] J. Hernandez, D. McDuff, and R. W. Picard, "Biowatch: Estimation of heart and breathing rates from wrist motions," in *Proc. 9th Int. Conf. Pervasive Comput. Technol. Healthcare (PervasiveHealth)*, May 2015, pp. 169–176.
- [7] R. Kukkapalli, N. Banerjee, R. Robucci, and Y. Kostov, "Micro-radar wearable respiration monitor," in *Proc. IEEE SENSORS*, Oct./Nov. 2016, pp. 1–3.
- [8] M. C. Huang *et al.*, "Inconspicuous on-bed respiratory rate monitoring," in *Proc. 6th Int. Conf. Pervasive Technol. Rel. Assistive Environ.*, May 2013, p. 18.
- [9] H. Abdelnasser, K. A. Harras, and M. Youssef, "UbiBreathe: A ubiquitous non-invasive WiFi-based breathing estimator," in *Proc. 16th ACM Int. Symp. Mobile Ad Hoc Netw. Comput.*, 2015, pp. 277–286.
- [10] V. Loon *et al.*, "Wireless non-invasive continuous respiratory monitoring with FMCW radar: A clinical validation study," *J. Clin. Monit. Comput.*, vol. 30, no. 6, pp. 797–805, 2016.
- [11] *ITU Towards 'IMT for 2020 and Beyond'—IMT-2020 Standards for 5G*, document, International Telecommunications Union, Feb. 2017. [Online]. Available: <https://www.itu.int/en/ITU-R/study-groups/rsg5/rwp5d/imt-2020/Pages/default.aspx>
- [12] A. Osseiran *et al.*, "Scenarios for 5G mobile and wireless communications: The vision of the METIS project," *IEEE Commun. Mag.*, vol. 52, no. 5, pp. 26–35, May 2014.
- [13] *Ministry of Industry and Information Technology on the Fifth Generation International Mobile Telecommunications System (IMT-2020) Using 3300–3600 MHz and 4800–5000 MHz Band Related Matters Notice*, Ministry Ind. Inf. Technol. People's Republic China, Beijing, China, Jun. 2017.
- [14] Y. Xiao, C. Li, and J. Lin, "A portable noncontact heartbeat and respiration monitoring system using 5-GHz radar," *IEEE Sensors J.*, vol. 7, no. 7, pp. 1042–1043, Jul. 2007.
- [15] C. Li, Y. Xiao, and J. Lin, "A 5GHz double-sideband radar sensor chip in 0.18 μm CMOS for non-contact vital sign detection," *IEEE Microw. Wireless Compon. Lett.*, vol. 18, no. 7, pp. 494–496, Jul. 2008.
- [16] I. Lawrence and K. Lin, "A concordance correlation coefficient to evaluate reproducibility," *Biometrics*, vol. 45, no. 1, pp. 255–268, Mar. 1989.
- [17] J. Benesty, J. Chen, Y. Huang, and I. Cohen, "Pearson correlation coefficient," in *Noise Reduction in Speech Processing*. Berlin, Germany: Springer, 2009, pp. 1–4.
- [18] Z. Yang, Z. Zhou, and Y. Liu, "From RSSI to CSI: Indoor localization via channel response," *ACM Comput. Surv.*, vol. 46, no. 2, pp. 25:1–25:32, Dec. 2013.
- [19] L. Davies and U. Gather, "The identification of multiple outliers," *J. Amer. Stat. Assoc.*, vol. 88, no. 423, pp. 782–792, 1993.
- [20] *Sleep Apnea: What is Sleep Apnea?*, NHLBI, Health Information for the Public, U.S. Dept. Health Human Services, Washington, DC, USA, Aug. 2016.